Chinese Journal of Cancer

Original Article

Suppressing tumor growth of nasopharyngeal carcinoma by hTERTC27 polypeptide delivered through adeno-associated virus plus adenovirus vector cocktail

Xiong Liu[1], Xiang-Ping Li[1], Ying Peng[2], Samuel S. Ng[3], Hong Yao[4], Zi-Feng Wang[3], Xiao-Mei Wang[5], Hsiang-Fu Kung[4] and Marie C.M. Lin[3]

Abstract

Nasopharyngeal carcinoma (NPC) is a metastatic carcinoma that is highly prevalent in Southeast Asia. Our laboratory has previously demonstrated that the C-terminal 27-kDa polypeptide of human telomerase reverse transcriptase (hTERTC27) inhibits the growth and tumorigenicity of human glioblastoma and melanoma cells. In this study, we investigated the antitumor effect of hTERTC27 in human C666-1 NPC cells xenografted in a nude mouse model. A cocktail of vectors comprising recombinant adeno-associated virus (rAAV) and recombinant adenovirus (rAdv) that each carry hTERTC27 (rAAV-hTERTC27 and rAdv-hTERTC27; the cocktail was abbreviated to rAAV/rAdv-hTERTC27) was more effective than either rAAV-hTERTC27 or rAdv-hTERTC27 alone in inhibiting the growth of C666-1 NPC xenografts. Furthermore, we established three tumors on each mouse and injected rAAV/rAdv-hTERTC27 into one tumor per mouse. Although hTERTC27 expression could only be detected in the injected tumors, reduced tumor growth was observed in the injected tumor as well as the uninjected tumors, demonstrating that the vector cocktail could provoke an antitumor effect on distant, metastasized tumors. Further studies showed the observed antitumor effects included inducing necrosis and apoptosis and reducing microvessel density. Together, our data suggest that the rAAV/rAdv-hTERTC27 cocktail can potently inhibit NPC tumor growth in both local and metastasized tumors and should be further developed as a novel gene therapy strategy for NPC.

Key words rAAV, Adv, nasopharyngeal carcinoma, hTERTC27

Nasopharyngeal carcinoma (NPC), a tumor derived from epithelial cells in the posterior nasopharynx, is highly prevalent in Southeast Asia. In 2000, more than 80% of new cases were reported in mainland China, Taiwan, Singapore, and other Asian countries and areas, with the highest incidence in southern China (25 to 30 cases per 100 000 people per year)[1-3]. In most of these populations, the male to female ratio is roughly 2–3 to 1[4]. The etiologic factors associated with endemic NPC include Epstein-Barr virus (EBV) infection (especially in type II and type III NPC), environmental factors (such as consumption of salted fish and preserved foods containing volatile nitrosamines), and genetic susceptibility[5]. Over 60% of NPC patients already have clinically detectable metastases in many distant organs at the time of diagnosis[6]. Although the local control rate for NPC is approaching 90%, 30%–40% of patients with advanced stage NPC subsequently develop distant metastases and/or local recurrences[7]. More importantly, the 5-year survival rate for patients with tumors >2 cm^3 is less than 50%[8], and most deaths are associated with secondary metastases to distant organs like the liver and lung. Once metastasis occurs, median survival is less than 12 months[9]. Therefore, developing novel treatment strategies for NPC metastasis is urgently needed.

Telomeres are DNA-protein complexes at the end of

Authors' Affiliations: [1]Department of Otolaryngology, Nanfang Hospital, Nanfang Medical University, Guangzhou, Guangdong 510515, P. R. China; [2]Department of Neurology, The Sun Yat-sen Memorial Hospital, Sun Yat-sen University, Guangzhou, Guangdong 510120, P. R. China; [3]Brain Tumor Center, Divison of Neurosurgery, Department of Surgery, The Chinese University of Hong Kong, Shatin, Hong Kong, China; [4]Center for Emerging Infectious Diseases, The Chinese University of Hong Kong, Shatin, Hong Kong, P. R. China; [5]Medical College, Shenzhen University, Shenzhen, Guangdong 518061, P. R. China.

Corresponding Author: Marie C.M. Lin, Brain Tumor Center, Divison of Neurosurgery, Department of Surgery, The Chinese University of Hong Kong, Shatin, Hong Kong, China. Tel: +852-26462713; Fax: +852-28171006; Email: mcllin@surgery.cuhk.edu.hk.

doi: 10.5732/cjc.011.10378

chromosomes that protect chromosomes from degradation and end-to-end fusion. Thus, telomeres are essential for genome stability and cell survival [10,11]. Telomerase activity is absent in most adult tissues; however, telomerase is reactivated in >85% of all human cancer cells[12,13]. High levels of telomerase activity were associated with poor prognosis of leukemia[14], neuroblastoma[15], and gastric cancer[16], whereas inhibition of telomerase was found to induce apoptosis in leukemia and colon cancer[14,16]. Telomerase expression was also reactivated in NPC biopsy samples[17].

Human telomerase reverse transcriptase (hTERT) is the catalytic subunit of telomerase and the rate-limiting component of the telomerase enzyme complex. The C-terminal 27-kDa polypeptide of hTERT (hTERTC27) consists of 251 amino acids and is highly divergent, with little or no obvious sequence conservation among different species[18,19]. In our previous studies, we demonstrated that ectopic overexpression of this polypeptide in hTERT-positive HeLa cells specifically caused telomere dysfunction and rapid chromosome end-fusion, resulting in cellular senescence and apoptosis[20]. Moreover, this occured without affecting the enzymatic activity of telomerase in the transfected cells[20,21]. These results suggest that hTERTC27 is a novel candidate for cancer gene therapy.

Various adenovirus (Adv) gene products can be used to enhance the transduction of adeno-associated virus (AAV)[22]. AAV was proposed to co-localize with adenovirus replication centers and use adenoviral and cellular proteins for its own replication[23]. However, Adv-mediated transgene expression is transient, and it causes dose-dependent toxicity[24] and activation of host immunity[25]. On the contrary, AAV has relatively low transduction efficiency, and it requires a larger amount of vectors and more time for transduction and transgene expression. Therefore, combination of Adv and AAV vectors not only reduces the side effects associated with Adv but also improves transduction efficiency of AAV. In this study, we constructed recombinant AAV (rAAV) and Adv (rAdv) vectors that expressed the hTERTC27 polypeptide (rAAV-hTERTC27 and rAdv-hTERTC27; the cocktail was abbreviated to rAAV/rAdv-hTERTC27) and investigated their effects and respective mechanisms of action in the treatment of NPC *in vivo*.

Materials and Methods

Cell lines and culture conditions

The EBV-positive NPC cell line C666-1 was kindly provided by Dr. Dolly P. Huang from the Chinese University of Hong Kong. The cells were cultured in RPMI-1640 with 10% fetal bovine serum in a humidified atmosphere containing 5% CO_2 at 37℃.

Materials

All rAAV and rAdv vectors were purchased from VGTC Company Limited (Beijing, China). CD31 (PECAM-1) antibody and horseradish peroxidase (HRP)-conjugated secondary antibody were purchased from Santa Cruz Biotechnology (USA). ApopTag® Peroxidase *In Situ* Apoptosis Detection Kit and EGFP monoclonal antibody were purchased from Chemicon (USA). TRIzol and the ThermoScript™ RT-PCR System (for cDNA transcripts) were purchased from Invitrogen (USA). HotstarTaq enzyme was purchased from Qiagen (USA).

Animal model and experimental conditions

Male nude mice (BALB/c *nu/nu*, 5–7 weeks old, weighing 15–22 g) were purchased from Charles River Laboratories (Wilmington, MA) and were cared according to the guidelines from the Laboratory Animal Unit of the University of Hong Kong. The first tumors were established by direct injection of 2×10^5 C666-1 cells subcutaneously on the right shoulder. The second and third tumors were also established at the same time by subcutaneous injection of same number of C666-1 cells on the left shoulder and haunch, respectively. When the tumors reached 3–4 mm in diameter, rAAV-hTERTC27 [1.5×10^{12} viral particles (v.p.)] and rAdv-hTERTC27 (2.5×10^8 pfu) were mixed, and the cocktail rAAV/rAdv-hTERTC27 was injected into the first tumors only. rAAV and rAdv expressing enhanced green fluorescent protein [rAAV-EGFP (1.5×10^{12} v.p.) and rAdv-EGFP (2.5×10^8 pfu)] were used in parallel as controls. Tumor volumes were measured every 5 days after injection. Mice were euthanized when the tumors were larger than 20 mm in diameter. Tumor samples were harvested for RT-PCR and immunohistochemical analysis. Liver and lung tissues were harvested, sectioned and then stained with hematoxylin and eosin (HE) for histological analyses to observe secondary metastasis.

To evaluate the infection efficiency of different groups—rAAV alone, rAdv alone, and rAAV and rAdv combined—we also established three tumors by direct injection of 2×10^5 C666-1 cells subcutaneously on the right shoulder (first tumor), left shoulder (second tumor), and haunch (third tumor). When the tumors reached 3–4 mm in diameter, rAAV-EGFP (1.5×10^{12} v.p.), Adv- EGFP (2.5×10^8 pfu), or a mixture of the two was injected into the first tumor. At 5 and 10 days after injection, mice were euthanized and tumors were fixed in 4% paraformaldehyde. The fixed tissues were embedded in paraffin, cut into 5-μm sections using a microtome, and subjected to immunohistochemical analysis.

RT-PCR

Tumor samples were freshly collected and stored in liquid nitrogen. Total RNA was extracted for reverse transcription-polymerase chain reaction (RT-PCR) (ThermoScript™ RT-PCR System) to evaluate the respective expression of *hTERTC27* and *EGFP*. *GAPDH* was used as loading control. RT-PCR products were visualized by agarose gel electrophoresis, and the relative mRNA level was determined using Gel-Pro Analyzer software (Media Cybernetics, Bethesda, MD).

Histology and TUNEL assay

Paraffin-embedded sections were deparaffinized with xylene, rehydrated with a graded series of ethanol, and then stained with H&E for histological studies or processed for terminal deoxynucleotidyltransferase-mediated dUTP-digoxigenin nick-end-labeling (TUNEL) assay (*In Situ* Cell Death Detection Kit, POD; Roche Applied Science, USA).

Immunohistochemical analysis

Paraffin-embedded tissue sections were dewaxed and rehydrated, and antigens were retrieved by heating the sections in 0.1 mol/L sodium citrate (buffer pH 6.0) for 10 min at 95℃ in the microwave. Sections were then treated with 3% H_2O_2 for 10 min and incubated with anti-EGFP primary antibody for 1 h. After being washed with PBS, sections were next incubated with HRP-conjugated secondary antibody for 30 min and stained with 3,3'-diaminobenzidine (DAB) substrate solution. Intratumoral microvessels were stained with a monoclonal antibody against CD31. Ten fields under 200× magnification were randomly chosen for each specimen. The number of EGFP-positive cells and microvessels formed were recorded.

Statistical analysis

Statistical analyses were performed using one-way ANOVA (SPSS 10.0, SPSS Inc., Chicago, IL). Values are expressed as mean ± standard deviation (SD). *P* values < 0.05 were considered statistically significant.

Results

The rAAV/rAdv vector cocktail induced strong expression of hTERTC27 and EGFP in C666-1 xenografts

Because an antibody against hTERTC27 is not commercially available and antibodies against the C-terminus of telomerase generate too many non-specific bands, we used RT-PCR to detect mRNA expression of *hTERTC27* in C666-1 xenografts in nude mice. As shown in Figures 1A and 1B, *EGFP* and *hTERTC27* mRNAs were expressed only in the treated first tumors but not in the untreated second or third tumors. Relatively stronger *hTERTC27* expression was detected at day 10 after injection.

We also used immunohistochemistry to confirm *in vivo* expression of EGFP after intratumoral injection of rAAV-EGFP, rAdv-EGFP, or the rAAV/rAdv-EGFP vector cocktail. As shown in Figure 1C, EGFP protein expression was detected in tumors injected with rAdv-EGFP alone and was markedly reduced at day 10 after injection. For rAAV-EGFP-injected tissues, however, no EGFP expression was observed 5 days after injection, but a high level of expression could be detected 10 days after injection. Importantly, the rAAV/rAdv-EGFP vector cocktail induced stronger EGFP expression at day 5 after injection than did either rAdv-EGFP or rAAV-EGFP alone.

rAAV-hTE1RTC27, rAdv-hTERTC27, and rAAV/rAdv-hTERTC27 significantly inhibited the growth of C666-1 tumor xenografts

As shown in Figure 2 and Table 1, rAAV/rAdv-hTERTC27 was more effective than either rAAV-hTERTC27 or rAdv-hTERTC27 alone in inhibiting NPC tumor growth in nude mice. Twenty days after injecting rAAV/rAdv-hTERTC27 into the first tumors, the volume of the first tumors (n = 12) was significantly smaller (P < 0.01) than that of uninjected second and third tumors (Figure 3 and Table 2). However, all tumors in the rAAV/rAdv-EGFP-injected groups had similar volumes. More importantly, complete tumor regression was found in 4 of 12 mice after injection of rAAV/rAdv-hTERTC27. Moreover, the volumes of second and third tumors from the rAAV/rAdv-hTERTC27-injected group were markedly smaller than those of the control rAAV/rAdv-EGFP-injected group (Figure 3 and Table 2), suggesting that the rAAV/rAdv-hTERTC27 vector cocktail inhibited the growth of both local and distant tumors.

No liver or lung metastasis was observed in C666-1 xenografts injected with rAAV/rAdv-hTERTC27

NPC is a highly malignant tumor that can easily invade local tissues and metastasize to distant organs. Because most deaths from NPC are associated with secondary metastases in distant organs, we investigated whether inoculation of NPC tumors in nude mice injected with rAAV/rAdv-hTERTC27 would induce secondary

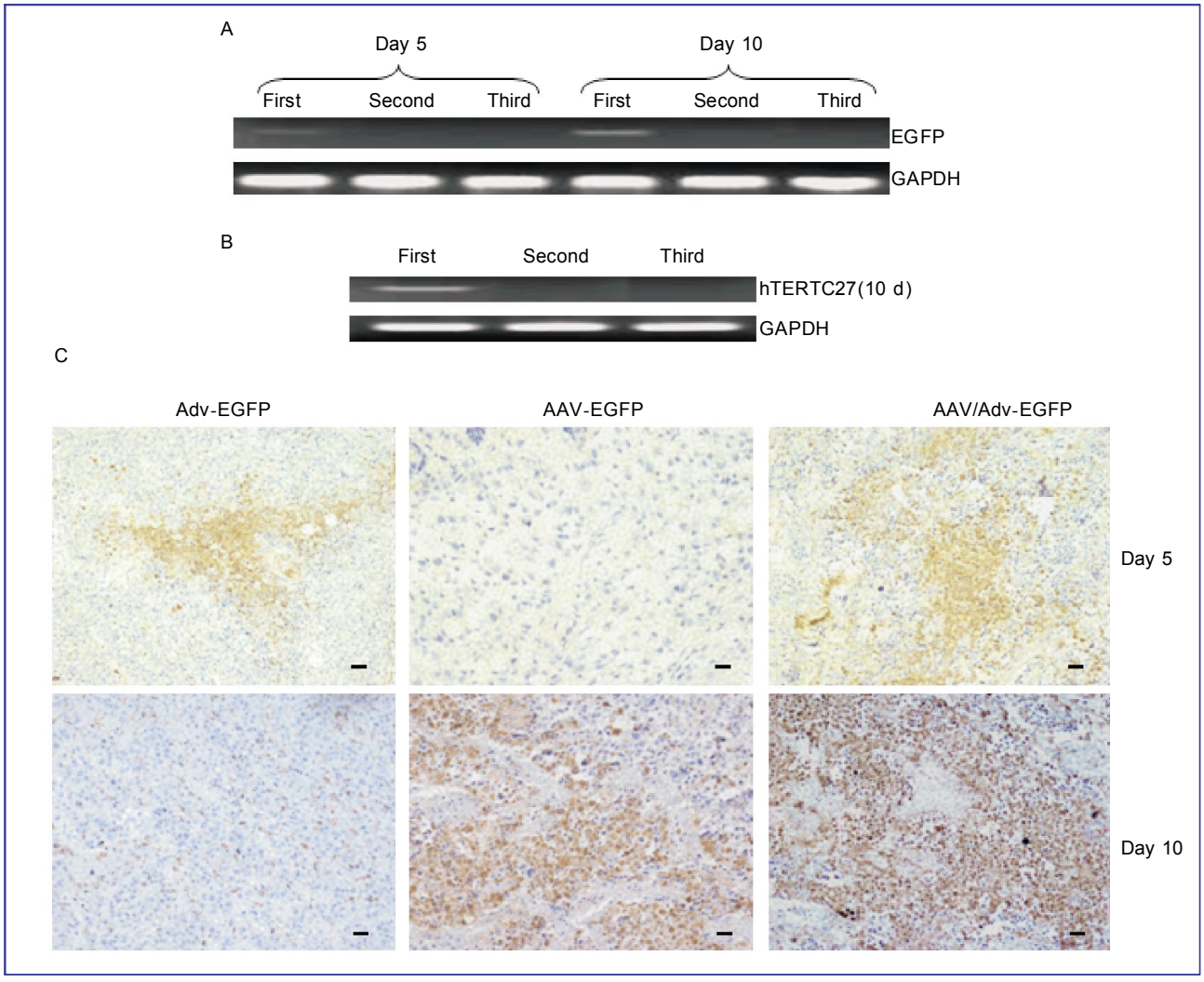

Figure 1. **rAAV- and rAdv-mediated expression of hTERTC27 or EGFP in nude mouse C666-1 xenografts.** A and B, reverse transcription-polymerase chain reaction (RT-PCR) analysis of EGFP (A) or hTERTC27 expression (B) in the first, second, or third tumors 5 or 10 days after injecting the rAAV/rAdv-hTERTC27 cocktail into the first tumor. C, immunohistochemical staining showing EGFP protein expression in nasopharyngeal carcinoma (NPC) tumors 5 days (top panels) or 10 days (bottom panels) after injection with rAdv-EGFP (left panels), rAAV-EGFP (middle panels), or rAAV/rAdv-EGFP (right panels). *Scale bars* = 30 μm.

metastases in the liver and lung. rAAV/rAdv-EGFP was used as a control. Mice were euthanized and their livers and lungs were collected when the tumors were larger than 20 mm in diameter. All livers and lungs appeared to be normal, and no secondary metastasis was observed in either the mice injected with rAAV/rAdv-hTERTC27 or rAAV/rAdv-EGFP (Figure 4).

rAAV/rAdv-hTERTC27 significantly decreased intratumoral vascularization

The microvessel density of each tumor was determined by immunohistochemical staining against CD31 (Figure 5). Very few new vessels were formed in the rAAV/rAdv-hTERTC27-injected first tumors as compared to the second and third tumors in the same injection group. In contrast, all tumors displayed similar levels of CD31 expression in the rAAV/rAdv-EGFP-injected group (Figure 5A). The average microvessel density of each tumor (Figure 5B) suggests that new vessels were scattered throughout the tumors. These data suggest that hTERTC27, when delivered by the rAAV/rAdv vector cocktail, effectively inhibits the growth of C666-1 cells through reduction of angiogenesis in nude mice.

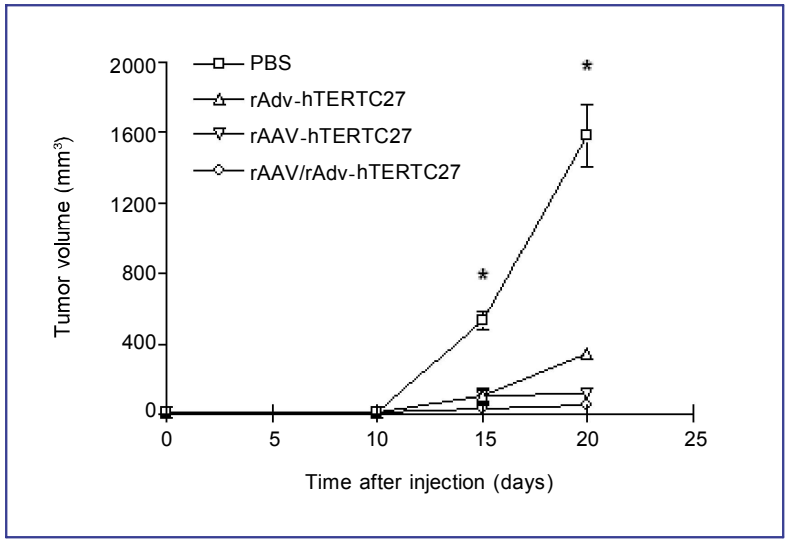

Figure 2. **NPC tumor volumes after intratumoral injection of PBS, rAdv-hTERTC27, rAAV-hTERTC27, or rAAV/rAdv-hTERTC27 in nude mice.** rAAV/rAdv-hTERTC27 is more effective than either rAAV-hTERTC27 or rAdv-hTERTC27 alone in inhibiting NPC tumor growth in nude mice. *$P < 0.05$.

Table 1. NPC tumor volumes at various time points in rAdv-hTERTC27-, rAAV-hTERTC27-, and rAAV/rAdv-hTERTC27-injected nude mice

Group	Tumor volume (mm^3)		
	Day 10	Day 15	Day 20
PBS	13.5 ± 2.1(4)	533.7 ± 105.4 (4)	1581.5 ± 352 (3)
rAdv-hTERTC27	12.1 ± 3.2 (4)	103.2 ± 92.5 [a] (4)	340.2 ± 48.1 [a] (3)
rAAV-hTERTC27	13.0 ± 2.1 (4)	107.5 ± 85.8 [a] (4)	117.5 ± 52 [a] (3)
rAAV/rAdv-hTERTC27	12.0 ± 1.3 (6)	33.5 ± 8.2 [b] (6)	57.1 ± 23.6 [b] (5)

Tumor volumes were measured 10, 15, and 20 days after injection. All values are presented as mean ± standard deviation. The numbers in parentheses indicate the number of mice. [a]$P < 0.05$, rAdv-hTERTC27 or rAAV-hTERTC27 versus PBS group, one-way ANOVA; [b]$P < 0.01$, rAAV/rAdv-hTERTC27 versus all other groups.

Table 2. NPC tumor volumes at various time points after injection of either rAAV/rAdv-EGFP or rAAV/rAdv-hTERTC27

Group	Tumor	Tumor volume (mm^3)			
		Day 10	15d (mm^3)	Day 20	Day 25
rAAV/rAdv-EGFP	First	12.0 ± 1.5	478.8 ± 124.7	1600.0 ± 520	
	Second	13.0 ± 1.8	511.5 ± 112.6	1647.7 ± 408	
	Third	13.0 ± 1.2	518.5 ± 150.1	1796.0 ± 588	
rAAV/rAdv-hTERTC27	First	12.0 ± 1.0	27.3 ± 15.1 [a]	71.3 ± 32.8 [a]	37.0 ± 8.0 [a]
	Second	13.0 ± 1.6	235.7 ± 89.2 [b]	635.8 ± 115.0 [b]	1236.0 ± 125.0
	Third	13.0 ± 1.3	272.3 ± 108.0 [b]	655.2 ± 171.8 [b]	1350.1 ± 243.0

Tumor volumes were measured 10, 15, 20, and 25 days after injection. All values are presented as mean ± standard deviation. The numbers in parentheses indicate the number of mice. [a]$P < 0.01$, first tumors versus second and third tumors in rAAV/rAdv-hTERTC27-injected mice, one-way ANOVA, $n = 12$; [b]$P < 0.05$, rAAV/rAdv-EGFP versus rAAV/rAdv-hTERTC27.

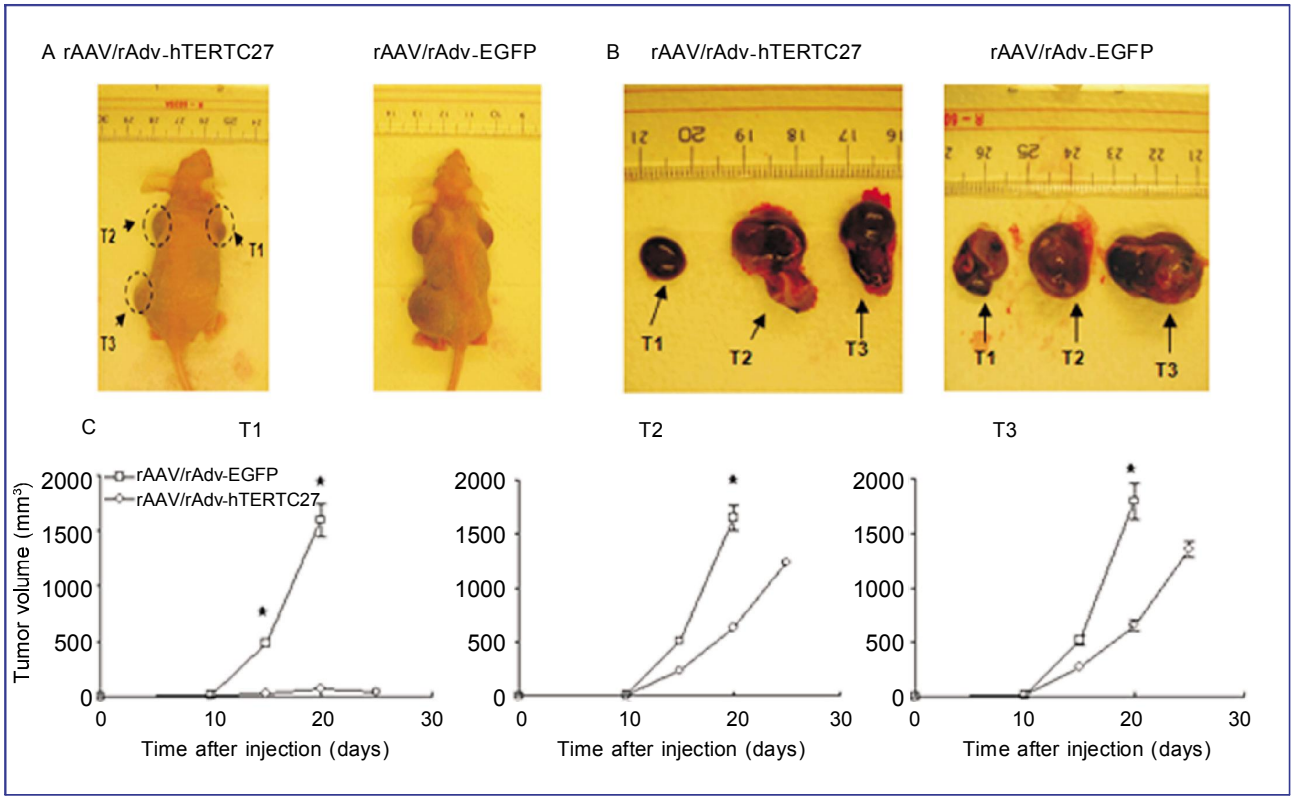

Figure 3. **NPC tumor volumes after injection with either rAAV/rAdv-EGFP or rAAV/rAdv-hTERTC27.** A, tumors in nude mice at 20 days after injection. B, tumors removed from nude mice at 20 days after injection. C, NPC tumor volumes at 10 and 20 days after injection. T1, first tumor; T2, second tumor; T3, third tumor. *, $P < 0.05$.

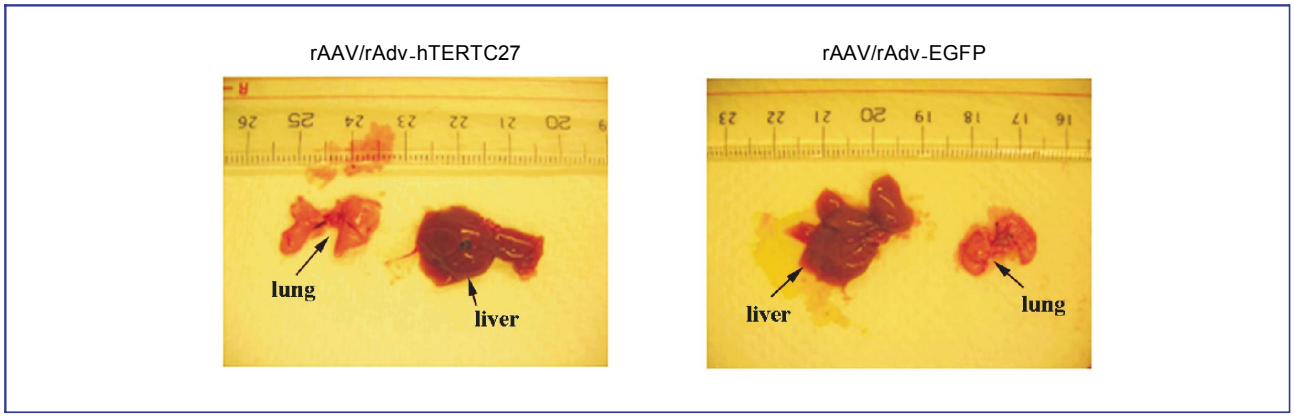

Figure 4. **Histological analysis of secondary metastasis of NPC xenografts in nude mice.** Representative pictures show the morphology of the liver and lung excised from mice injected with rAAV/rAdv-hTERTC27 or rAAV/rAdv-EGFP.

rAAV/rAdv-hTERTC27 induced necrosis and apoptosis in the injected but not the uninjected tumors

In HE-stained sections, necrosis was observed in the first tumors that injected with rAAV/rAdv-hTERTC27 (Figure 6A, dotted circle on the upper left panel), but not in the second and third tumors within the same group or in any of the tumors from the control group (Figure 6A). Apoptosis was also evaluated in C666-1 xenografts with

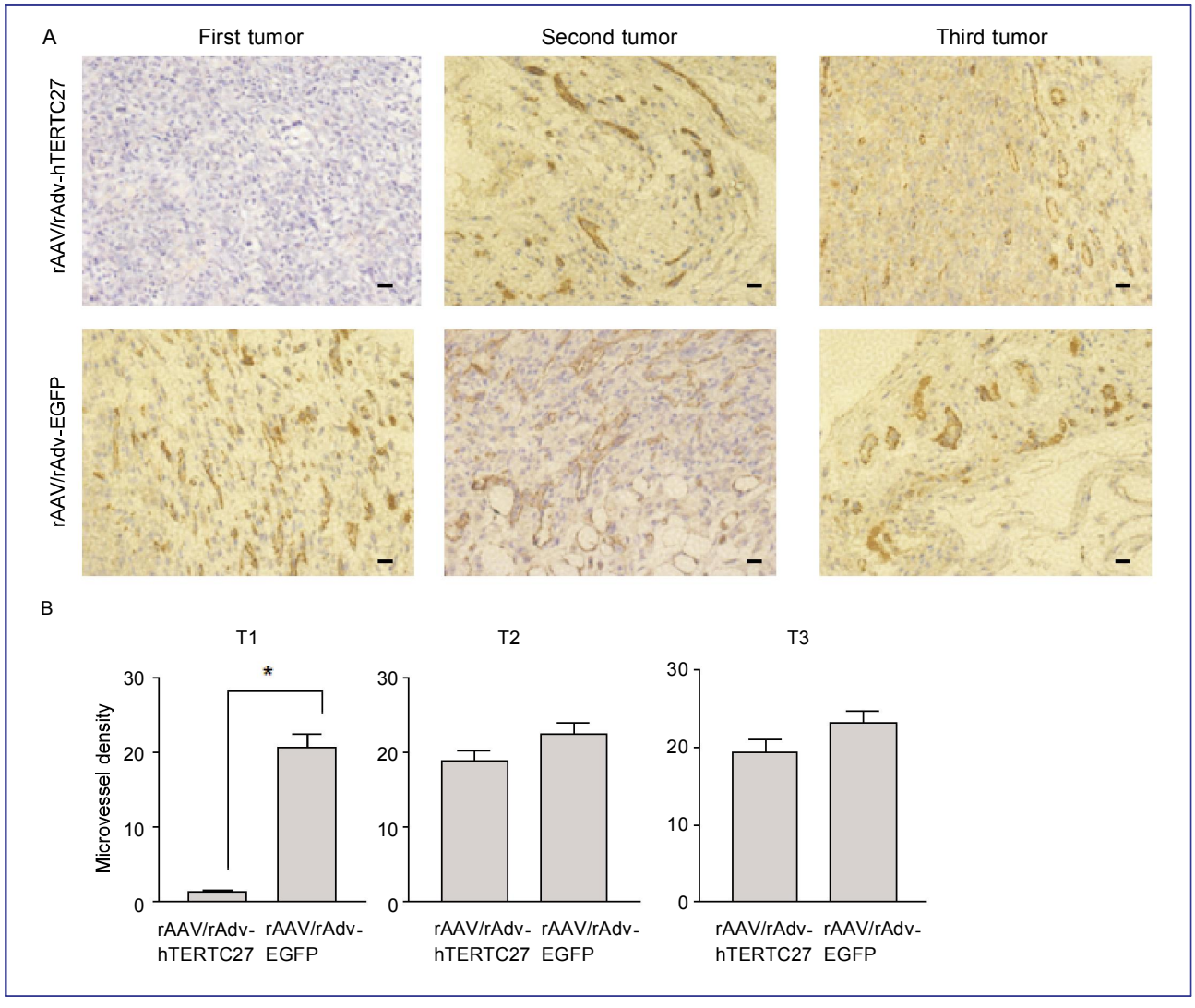

Figure 5. **Microvessel density of NPC tumor tissues as revealed by immunohistochemical staining of CD31.** A. CD31 staining of the first, second, and third tumors isolated from rAAV/rAdv-hTERTC27-injected or rAAV/rAdv-EGFP-injected mice. *Scale bars* = 30 μm. B, the mean number of microvessels in the first (T1), second (T2), and third (T3) tumors 10 days after rAAV/rAdv-hTERTC27 or rAAV/rAdv-EGFP injection in the first tumors. The data are averages from 10 visual fields. $^*P < 0.05$.

the TUNEL assay. The results revealed that rAAV/rAdv-hTERTC27 induced apoptosis in the injected NPC tumors, but not in the uninjected tumors or the tumors in the control rAAV/rAdv-EGFP-injected groups (Figure 6B). As shown in Figure 6C, the average number of apoptotic cells was higher in tumors injected with rAAV/rAdv-hTERTC27 than in tumors that were not injected or in tunors injected with rAAV/rAdv-EGFP.

Discussion

Immunohistochemistry revealed that rAdv-mediated target gene expression could reach a very high level in a short time; however, this expression did not last long (~5 days after injection). In contrast, rAAV-mediated transgene expression was maintained at a high level for an extended period of time but took about 5 days to reach maximum expression. Therefore, we employed a vector cocktail, a combination of rAdv and rAAV, to resolve the limitations of using either rAdv or rAAV alone. The vector cocktail comprising rAAV and rAdv carrying hTERTC27 (rAAV/rAdv-hTERTC27) was more effective than either rAAV-hTERTC27 or rAdv-hTERTC27 alone in inhibiting the growth of C666-1 NPC

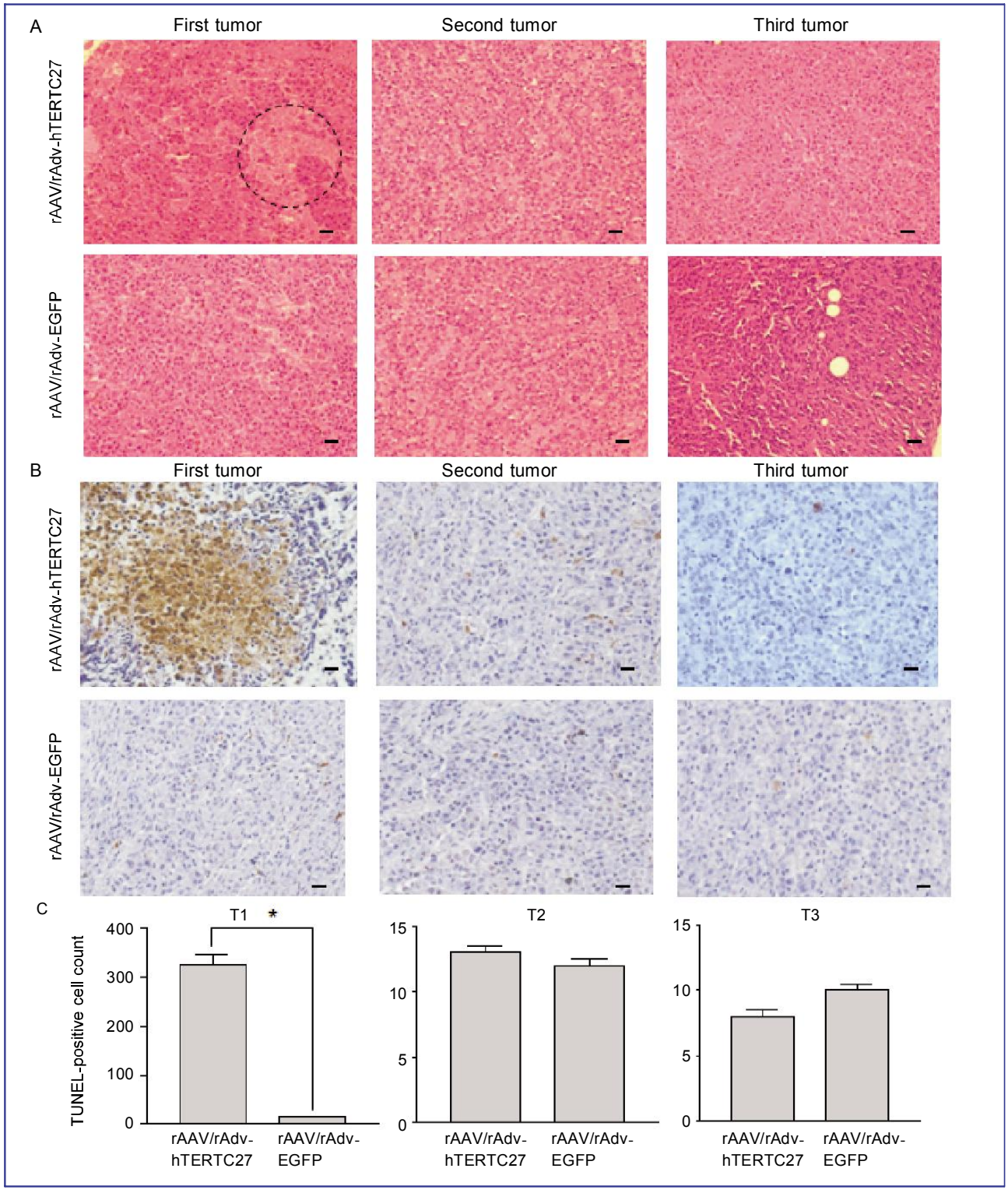

Figure 6. **Necrosis and apoptosis in tumor tissues after injection of rAAV/rAdv-hTERTC27 or rAAV/rAdv-EGFP.** A, HE-stained tissue sections of NPC xenografts injected with rAAV/rAdv-hTERTC27 or rAAV/rAdv-EGFP. B, TUNEL assay on NPC xenografts injected with rAAV/rAdv-hTERTC27 or rAAV/rAdv-EGFP. A large number of TUNEL-positive cells (in brown) are detected in first tumors. Scale bars = 30 μm. C, the mean number of TUNEL-positive cells in the first (T1), second (T2), and third (T3) tumors 10 days after injection of rAAV/rAdv-hTERTC27 or rAAV/rAdv-EGFP in the first tumor. The data are averages from 5 visual fields. $^*P < 0.05$.

xenografts when injected intratumorally into nude mice. Furthermore, we demonstrated that the vector cocktail could provoke a distant antitumor effect on metastasized tumors. rAAV/rAdv-hTERTC27 significantly decreased intratumoral vascularization and induced necrosis and apoptosis in the injected but not the uninjected tumors.

In this study, three tumors were established subcutaneously in each nude mouse, and only one tumor was injected with the rAAV/rAdv-hTERTC27 vector cocktail. Our results showed that expression of hTERTC27 could only be detected in the injected tumors, but not in the uninjected second or third tumors. hTERTC27 expression was observed as early as 5 days after injection and was maintained up to 10 days after injection. Importantly, complete tumor regression was found in 4 of 12 rAAV/rAdv-hTERTC27-injected mice, consistent with the observation that the vector cocktail was more effective than either rAAV-hTERTC27 or rAdv-hTERTC27 alone in inhibiting the growth of NPC xenografts. Moreover, rAAV/rAdv-hTERTC27 vector cocktail reduced the growth of distant uninjected tumors, suggesting that it mediates a distant bystander effect. This finding is in agreement with our hypothesis that hTERTC27 elicits a tumor-specific immune response[26,27]. Consistent with our data in glioblastoma and melanoma xenografts[26,27], immunohistochemical staining revealed that microvessel density was markedly reduced and that both necrosis and apoptosis were induced in tumors expressing hTERTC27, suggesting that the antitumor activities of hTERTC27 are elicited by multiple mechanisms.

The molecular mechanism by which hTERTC27 inhibits NPC tumor growth remains unclear. Our previous studies have demonstrated that hTERTC27 expression leads to telomere dysfunction, suppresses the growth and tumorigenicity of HeLa cells, and sensitizes HeLa cells to H_2O_2-induced senescence[20,21]. Because these phenomena occur without affecting the enzymatic activity of telomerase, the alternative lengthening of telomeres (ALT) mechanism is likely to be suppressed, thereby inducing the antitumor activity of hTERTC27 in NPC. The ALT mechanism, wherein telomeres are maintained by a recombination-based pathway, was found to be activated in telomerase-negative human cancer cells[28-30]. Ectopic overexpression of hTERT was sufficient to allow T-Ag-transformed human embryonic kidney cells to bypass crisis; however, when an HA epitope tag was added to the C-terminus of hTERT (hTERT-HA), this effect was lost. The hTERT-HA-transfected cells continued to lose telomeric DNA and ceased to proliferate [31,32]. We therefore hypothesize that overexpression of hTERTC27 may inhibit ALT and lead to telomere shortening, which in turn results in apoptosis and necrosis in NPC cells.

To our knowledge, this is the first report demonstrating that rAAV and rAdv expressing the hTERT C-terminal polypeptide fragment exerted potent anti-NPC effects *in vivo*. These effects are mediated through induction of necrosis and apoptosis and suppression of angiogenesis. These results, in addition to results from our previous studies, suggest that therapy with this rAAV/rAdv-hTERTC27 vector cocktail is a novel and promising clinical strategy for NPC as well as other tumors.

Acknowledgments

The authors thank Professor Dolly Huang for generously providing the C666-1 cell line, and thank Drs. Ming Li, Gao Yi, and Mr. David Chau for discussions and critical review of this paper.

Received: 2011-09-29; revised: 2012-09-04;
accepted: 2012-09-21.

References

[1] McDermott AL, Dutt SN, Watkinson JC. The aetiology of nasopharyngeal carcinoma. Clin Otolaryngol Allied Sci, 2001,26:82–92.
[2] Tao Q, Chan AT. Nasopharyngeal carcinoma: molecular pathogenesis and therapeutic developments. Expert Rev Mol Med, 2007,9:1–24.
[3] Chang ET, Adami HO. The enigmatic epidemiology of nasopharyngeal carcinoma. Cancer Epidemiol Biomarkers Prev, 2006,15:1765–1777.
[4] Yu MC, Yuan JM. Epidemiology of nasopharyngeal carcinoma. Semin Cancer Biol, 2002,12:421–429.
[5] Vokes EE, Liebowitz DN, Weichselbaum RR. Nasopharyngeal carcinoma. Lancet, 1997,350:1087–1091.
[6] Hu LF, Chen F, Zheng X, et al. Clonability and tumorigenicity of human epithelial cells expressing the EBV encoded membrane protein LMP1. Oncogene, 1993,8:1575–1583.
[7] Teo PM, Chan AT. Treatment strategy and clinical experience. Semin Cancer Biol, 2002,12:497–504.
[8] Busson P, Keryer C, Ooka T, et al. EBV-associated nasopharyngeal carcinomas: from epidemiology to virus-targeting strategies. Trends Microbiol, 2004,12:356–360.
[9] Ma BB, Chan AT. Recent perspectives in the role of chemotherapy in the management of advanced nasopharyngeal carcinoma. Cancer, 2005,103:22–31.
[10] Blackburn EH. The end of the (DNA) line. Nat Struct Biol, 2000,7:847–50.
[11] Counter CM, Avilion AA, Lefeuvre CE, et al. Telomere shortening associated with chromosome instability is arrested in immortal cells which express telomerase activity. EMBO J, 1992,11:1921–1929.
[12] Shay JW, Zou Y, Hiyama E, et al. Telomerase and cancer. Hum Mol Genet, 2001,10:677–685.

[13] Shay JW, Bacchetti S. A survey of telomerase activity in human cancer. Eur J Cancer, 1997,33:787–791.
[14] Bechter OE, Eisterer W, Pall G, et al. Telomere length and telomerase activity predict survival in patients with B cell chronic lymphocytic leukemia. Cancer Res, 1998,58:4918–4922.
[15] Hiyama E, Hiyama K, Ohtsu K, et al. Telomerase activity in neuroblastoma: is it a prognostic indicator of clinical behaviour? Eur J Cancer, 1997,33:1932–1936.
[16] Hiyama E, Yokoyama T, Tatsumoto N, et al. Telomerase activity in gastric cancer. Cancer Res, 1995,55:3258–3262.
[17] Wen Z, Xiao J, Tang F, et al. Expression of telomerase and its RNA in nasopharyngeal carcinoma. Chin Med J (Engl), 2000,113:525–528.
[18] Friedman KL, Cech TR. Essential functions of amino-terminal domains in the yeast telomerase catalytic subunit revealed by selection for viable mutants. Genes Dev, 1999,13:2863–2874.
[19] Lai CK, Mitchell JR, Collins K. RNA binding domain of telomerase reverse transcriptase. Mol Cell Biol, 2001,21:990–1000.
[20] Huang JJ, Lin MC, Bai YX, et al. Ectopic expression of a COOH-terminal fragment of the human telomerase reverse transcriptase leads to telomere dysfunction and reduction of growth and tumorigenicity in HeLa cells. Cancer Res, 2002,62:3226–3232.
[21] Huang JJ, Bai YX, Han SW, et al. A human TERT C-terminal polypeptide sensitizes HeLa cells to H_2O_2-induced senescence without affecting telomerase enzymatic activity. Biochem Biophys Res Commun, 2003,301:627–632.
[22] Fisher KJ, Gao GP, Weitzman MD, et al. Transduction with recombinant adeno-associated virus for gene therapy is limited by leading-strand synthesis. J Virol, 1996,70:520–532.
[23] Weitzman MD, Fisher KJ, Wilson JM. Recruitment of wild-type and recombinant adeno-associated virus into adenovirus replication centers. J Virol, 1996,70:1845–1854.
[24] Wen XY, Bai YH, Stewart K. Adenovirus-mediated human endostatin gene delivery demonstrates strain-specific antitumor activity and acute dose-dependent toxicity in mice. Hum Gene Ther, 2001,12:347–358.
[25] Jooss K, Ertl HCJ, Wilson JM. Cytotoxic T-lymphocyte target proteins and their major histocompatibility complex class I restriction in response to adenovirus vectors delivered to mouse liver. J Virol, 1998,72:2945–2954.
[26] Ng SS, Gao Y, Chau DH, et al. A novel glioblastoma cancer gene therapy using AAV-mediated long-term expression of human TERT C-terminal polypeptide. Cancer Gene Ther, 2007,14:561–572.
[27] Huo LF, Yao H, Wang XC, et al. Inhibition of melanoma growth by subcutaneous administration of hTERTC27 viral cocktail in C57BL/6 mice. PLoS One, 2010,5:e12705.
[28] Bryan TM, Englezou A, Gupta J, et al. Telomere elongation in immortal human cells without detectable telomerase activity. EMBO J, 1995,14:4240–4248.
[29] Bryan TM, Englezou A, DallaPozza L, et al. Evidence for an alternative mechanism for maintaining telomere length in human tumors and tumor-derived cell lines. Nat Med, 1997,3:1271–1274.
[30] Dunham MA, Neumann AA, Fasching CL, et al. Telomere maintenance by recombination in human cells. Nat Genet, 2000,26:447–450.
[31] Wu KJ, Grandori C, Amacker M, et al. Direct activation of TERT transcription by c-MYC. Nat Genet, 1999,21:220–224.
[32] Counter CM, Hahn WC, Wei WY, et al. Dissociation among *in vitro* telomerase activity, telomere maintenance, and cellular immortalization. Proc Natl Acad Sci U S A, 1998,95:14723–14728.